

Chapter 8

Blue Light Chargeable Persistent Phosphors

Jumpei Ueda

Abstract Persistent phosphors are materials that show continuous luminescence for a long duration, from several minutes to a few hours after ceasing the excitation light. They have been used in luminous paints in indoor and outdoor environments, for emergency signs, watch dials, etc. In this chapter, the history of persistent phosphors and the persistent luminescence mechanism are described, and our new persistent phosphors are introduced. In 2013, a blue light chargeable persistent phosphor, $Y_3Al_{5-x}Ga_xO_{12}:Ce^{3+}-Cr^{3+}$, was successfully developed by our research group on the basis of material design for persistent phosphors; this has also been explained in the text. For the charging process, the relative energy location between the excited $Ce^{3+}:5d$ level and the bottom of the conduction band was controlled by bandgap engineering. In addition, Cr ions were co-doped into the bandgap engineered $Y_3Al_{5-x}Ga_xO_{12}:Ce^{3+}$ phosphor to form numerous electron traps. The detailed properties of $Y_3Al_{5-x}Ga_xO_{12}:Ce^{3+}-Cr^{3+}$ for the charging and de-charging processes were analyzed by thermoluminescence measurements. Tuning of the persistent luminescence color is also discussed.

8.1 History of Persistent Phosphors

Persistent phosphors show continuous luminescence for a long duration ranging from several minutes to a few hours even after the excitation light source is removed, as opposed to phosphors that show luminescence with a decay time

on the nanosecond and millisecond scale because of intrinsic ion transitions. Persistent phosphors have found application in luminous paints in indoor and outdoor environments, for emergency signs, clock dials, and glow-in-the-dark road marks.

The first persistent phosphor to be reported was Bologna Stone, prepared by Vincenzo Casciarolo in 1602 (Yen, 2007). Bologna Stone shows persistent red luminescence after illumination by sunlight. The composition of this phosphor is BaS:Cu⁺, and the luminescence originates from the Cu⁺: 3d⁹4s → 3d¹⁰ transition (Lin, 2001; Lastusaari, 2012). Upon its discovery, the then-novel Bologna stone attracted the interest of scientists and the public because of its aesthetic value and potential utility in lighting.

From the 1900s, persistent phosphors have been used for practical applications, i.e., in luminous paints for dials of clocks and watches. Until the 1990s, radioactive elements such as radium, tritium, and promethium were added to green phosphors based on ZnS because storage-type persistent phosphors with non-radioactive elements, such as ZnS:Cu, showed insufficient brightness and short persistent luminescence. In storage-type persistent phosphors, temporary photoionized electrons from the luminescence center upon illumination by high-energy light are trapped in the defects of the host. Once the light source is removed, the trapped electrons are released thermally and transferred to the photo-oxidized luminescence center for recombination. On the other hand, persistent phosphors with radioactive ions can be continually excited by α - and β -rays produced by radioactive decay of the radioactive ion; hence, the phosphor shows much brighter persistent luminescence.

However, by the 1990s, there was increased public concern regarding the health hazards and environmental pollution caused by radioactive elements. In addition, there was a decrease in the annual sales of watches with persistent phosphors based on radioactive elements, while the demand for clocks with the storage-type persistent phosphors increased despite the relatively low persistent luminance. From these reasons, Nemoto & Co., Ltd., which deals with the development, manufacture, and sales of persistent phosphors in Japan, decided to develop high-luminance persistent phosphors without using radioactive ions in early 1991 (Murayama, 2007). The project team (Project Leader: T. Matsuzawa; Research Chief: Y. Aoki) commenced work on the development of persistent phosphors based on aluminate oxide. Finally, Aoki developed a new persistent phosphor, SrAl₂O₄:Eu²⁺-Dy³⁺, on March 12, 1993 (Murayama, 2007; Murayama, 1995; Matsuzawa, 1995). SrAl₂O₄:Eu²⁺-Dy³⁺ showed ten-fold higher brightness and duration as compared to ZnS-based persistent phosphors. The development of SrAl₂O₄:Eu²⁺-Dy³⁺ was a breakthrough in the field of persistent phosphors, and this phosphor rapidly replaced ZnS-based persistent phosphors that were in use for almost a century.

8.2 Mechanism Underlying the Action of Persistent Phosphor, $\text{SrAl}_2\text{O}_4:\text{Eu}^{2+}\text{-Dy}^{3+}$

Following the discovery of $\text{SrAl}_2\text{O}_4:\text{Eu}^{2+}\text{-Dy}^{3+}$, several researchers became interested in the mechanism underlying the persistent luminescence. The project team at Nemoto & Co., Ltd., also discussed the persistent luminescence mechanism in their original paper in 1996 (Matsuzawa, 1996). The mechanism was explained by a hole capture model: when the Eu^{2+} ion is excited, a hole escapes to the valence band ($\text{Eu}^{2+} \rightarrow \text{Eu}^+$), and is trapped by Dy^{3+} ($\text{Dy}^{3+} \rightarrow \text{Dy}^{4+}$) as shown in Fig. 8.1 (left). The trapped hole can be thermally released, resulting in persistent luminescence. In another paper published in the same year, Takasaki and Tanabe suggested that the excited electron from the Eu^{2+} ion is transferred to the conduction band (CB) and is trapped by Dy^{3+} as shown in Fig. 8.1 (right). This proposal is also based on an empirical fact that Eu^+ and Dy^{4+} are energetically unstable, and is thus non-plausible (Takasaki, 1996). The Matsuzawa model has often been used to explain the mechanism of persistent luminescence

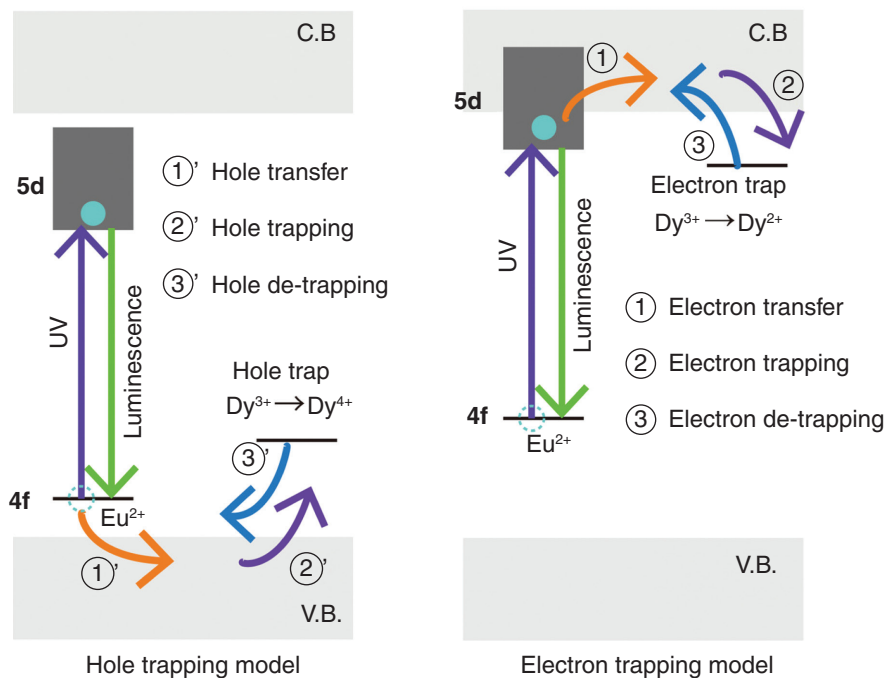


Fig. 8.1 Schematic representation of mechanism underlying persistent luminescence in $\text{SrAl}_2\text{O}_4:\text{Eu}^{2+}\text{-Dy}^{3+}$ based on (left) hole trapping and (right) electron trapping models

cence in $\text{SrAl}_2\text{O}_4:\text{Eu}^{2+}\text{-Dy}^{3+}$ and other new materials of this type. Recently, the electron trap model based on Dy^{3+} was widely accepted with the explanation using the “Dorenbos model,” which gives the electronic energy level positions of the lanthanide ions relative to the valence band and CB in some host materials (Dorenbos, 2005). Electron charging in $\text{SrAl}_2\text{O}_4:\text{Eu}^{2+}\text{-Dy}^{3+}$ by UV and blue light excitation was also discussed by our research group on the basis of the excitation wavelength and temperature dependence of photoconductivity. The lowest excited 5d level was found to be located 0.34 eV below the bottom of the CB (Ueda, 2012).

8.3 New Demand for Persistent Phosphors

Almost all bright and long persistent storage-type phosphors show green and blue luminescence, for example, $\text{SrAl}_2\text{O}_4:\text{Eu}^{2+}\text{-Dy}^{3+}$ ($\lambda_{\text{em}} = 510$ nm) (Yen, 2007), $\text{CaAl}_2\text{O}_4:\text{Eu}^{2+}\text{-Nd}^{3+}$ ($\lambda_{\text{em}} = 440$ nm) (Matsuzawa, 1996), $\text{Sr}_4\text{Al}_{14}\text{O}_{25}:\text{Eu}^{2+}\text{-Dy}^{3+}$ ($\lambda_{\text{em}} = 490$ nm) (Aoki, 1997; Lin, 2001a; Lin, 2002), and $\text{Sr}_2\text{MgSi}_2\text{O}_7:\text{Eu}^{2+}\text{-Dy}^{3+}$ ($\lambda_{\text{em}} = 470$ nm) (Lin, 2001b), as shown in Fig. 8.2. Some red persistent phosphors are known, but they have not been commercialized because of their low

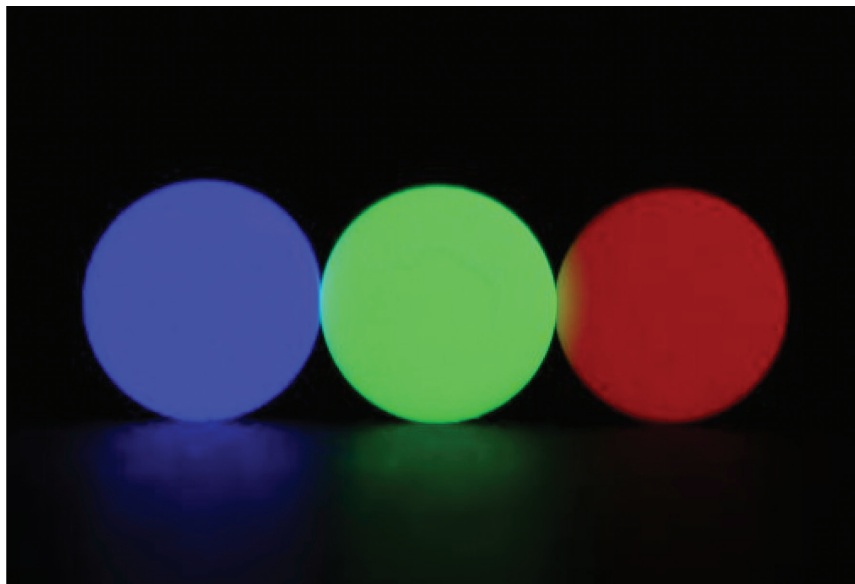


Fig. 8.2 Images of persistent phosphors (blue, $\text{CaAl}_2\text{O}_4:\text{Eu}^{2+}\text{-Nd}^{3+}$; green, $\text{SrAl}_2\text{O}_4:\text{Eu}^{2+}\text{-Dy}^{3+}$; red, $\text{MgGeO}_3:\text{Mn}^{2+}\text{-Yb}^{3+}$)

luminescence intensity, short duration of persistent luminescence, hygroscopic nature of the host material, and short charging wavelength ($\lambda_{ex} = 250$ nm). Among them, $\text{SrAl}_2\text{O}_4:\text{Eu}^{2+}\text{-Dy}^{3+}$ and $\text{Sr}_4\text{Al}_{14}\text{O}_{25}:\text{Eu}^{2+}\text{-Dy}^{3+}$ are practically used because of their brighter persistent luminance and better chemical stability. These practical persistent phosphors are used in daily life. Fig. 8.3 shows the image of a luminous signature in Tokyo Metro. The luminous signature is visible even in the dark, as shown in the inset of Fig. 8.3. Blue and green persistent phosphors usually show the best performance for persistent luminescence under UV and violet-light excitation from a reliable source, such as a fluorescent lamp (Takasaki, 1996; Bos, 2011).

Currently, white-light emitting diodes (w-LEDs), consisting of blue-LEDs and $\text{Y}_3\text{Al}_5\text{O}_{12}(\text{YAG}):\text{Ce}^{3+}$ yellow phosphors, are increasingly being used as replacements to fluorescent lamps for indoor illumination because of their high luminous efficiency, long lifetime, and energy-saving capability. Moreover, for the use of persistent phosphors in outdoor environments, persistent luminescence must be induced not only by UV and violet light, but also by longer-wavelength



Fig. 8.3 Image of luminous signature in Tokyo Metro. (inset) Enlarged image in a dark atmosphere

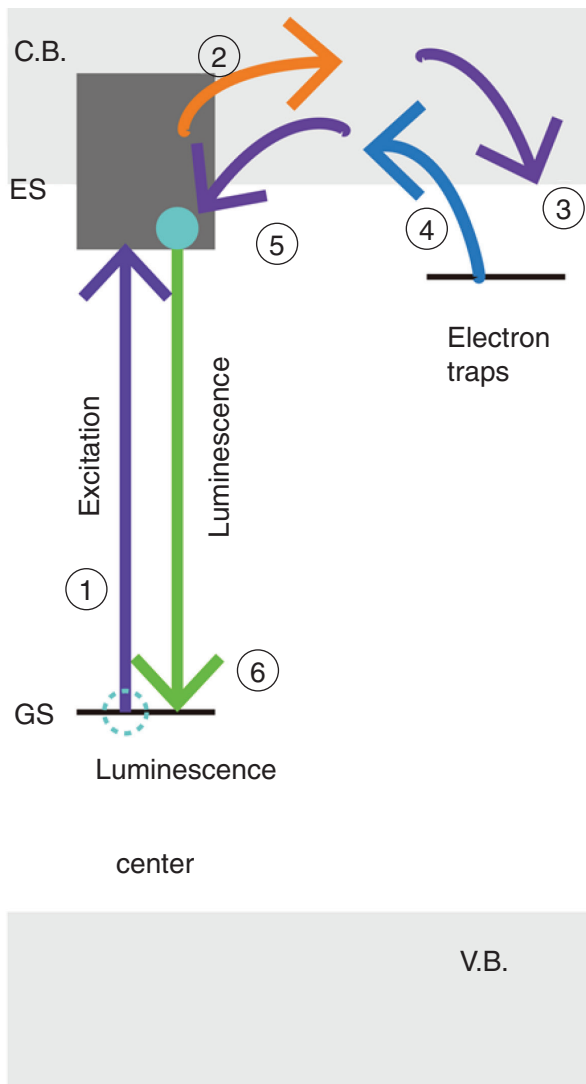


Fig. 8.4 General mechanism for persistent luminescence

light such as blue light, because the sunlight spectrum shows a peak at around 500 nm and the UV intensity is weaker than the visible-light intensity. Therefore, blue-light-induced persistent luminescence materials showing yellow to red luminescence have been the focus of considerable development.

8.4 Strategy for Developing New Persistent Phosphors

Persistent luminescence is caused by the following sequence of events (Fig. 8.4): 1) excitation of luminescent centers; 2) thermal ionization of excited electrons to the CB; 3) capture of electrons in the CB by traps (trapping); 4) gradual release of electrons in the traps by thermal energy (de-trapping); 5) transfer of de-trapped electrons to the photo-oxidized luminescent centers, resulting in luminescence. Therefore, to design a persistent phosphor, it is necessary to control the relative energy locations of the excited state, traps, and CB. For effective charging, the energy gap between the excited state and the CB should be small, and for the de-trapping process, the trap depth should be optimized to release electrons from the traps at room temperature. In addition, to develop blue light chargeable persistent phosphors, we must select a phosphor that shows strong blue light absorption and visible luminescence.

Recently, by controlling the relative energy location, we successfully developed a new Ce³⁺-doped garnet persistent phosphor showing Ce³⁺:5d-4f green luminescence ($\lambda_{em} = 505$ nm) that persists for several hours after blue-light excitation (Ueda, 2014, b).

8.5 Ce³⁺-Doped Garnet Phosphors

Ce³⁺-doped garnet materials have attracted a great deal of attention for application in w-LEDs and scintillators because of their intense broad absorption in the blue region, high quantum efficiency, and multicolor luminescence. These absorption and luminescence properties of the Ce³⁺ ion are responsible for the *4f-5d* allowed transitions. The luminescence color variation is caused by shifting of the *5d* excited level by the nephelauxetic effect (centroid shift caused by covalence) and crystal field splitting, both of which strongly depend on the host crystals (Dorenbos, 2000a; Dorenbos, 2000b; Dorenbos, 2001; Dorenbos, 2002), as shown in Fig. 8.5. The chemical formula of general garnet crystals is $\{A\}_3[B]_2(C)_3O_{12}$, where $\{A\}$, $[B]$, and (C) represent the cations at the dodecahedral, octahedral, and tetrahedral sites, respectively, as shown in Fig. 8.6. The crystal field splitting strength is controlled by changing the garnet component ions. This is because the garnet structure has three cation sites that can be occupied by various cations. The dodecahedral site that Ce³⁺ occupies has a distorted square anti-prism structure with D₂ point-group symmetry and its distortion can be affected by the garnet composition. The optical properties of Ce³⁺ in many garnet host compositions have been studied thus far. For instance, the dodecahedral $\{A\}$ sites can be substituted by relatively large rare earth ions

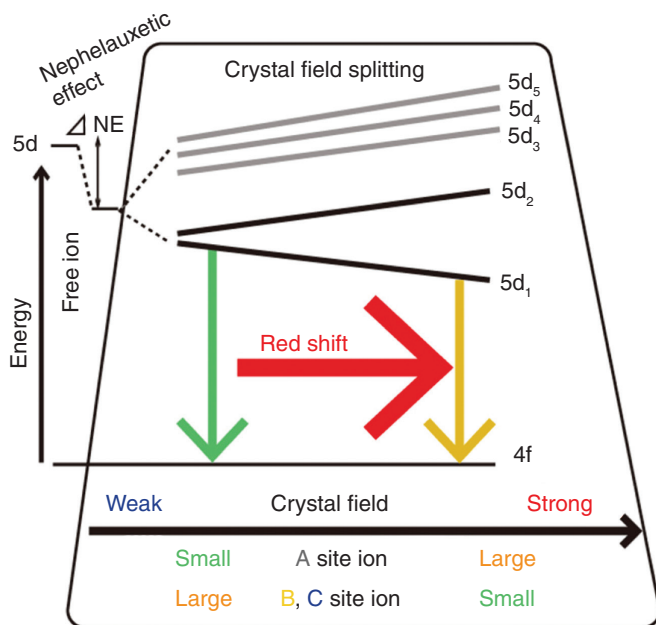


Fig. 8.5 Schematic diagram of the 5d energy level

(La, Gd, Tb, Y, Lu) and alkali-earth ions (Mg, Ca); [B] sites can be substituted by small rare earth ions (Y, Lu, Sc) and some metal ions (In, Ga, Al); (C) sites can be substituted by small metal ions (Ga, Al, Ge, Si) (Holloway, 1969; Tien, 1973; Zorenko, 2007; Korzhik, 1995; Ueda, 2011; Shimizu, 2012; Ueda, 2013; Jiang, 2010; Setlur, 2006; Gundiah, 2007). Consequently, Ce³⁺-doped garnet solid solutions show luminescence in various colors, from bluish green to orange.

8.6 Ce³⁺-Doped Garnet Persistent Phosphors

The optical properties of Ce³⁺-doped garnet materials, such as blue excitation and multicolor luminescence in the visible region, are also suitable for persistent phosphors. However, there are very few reports on intense persistent luminescence in Ce³⁺-doped garnet materials till date. This is because the relative energy location of the 5d excited state, trap, and CB has not been optimized for persistent luminescence.

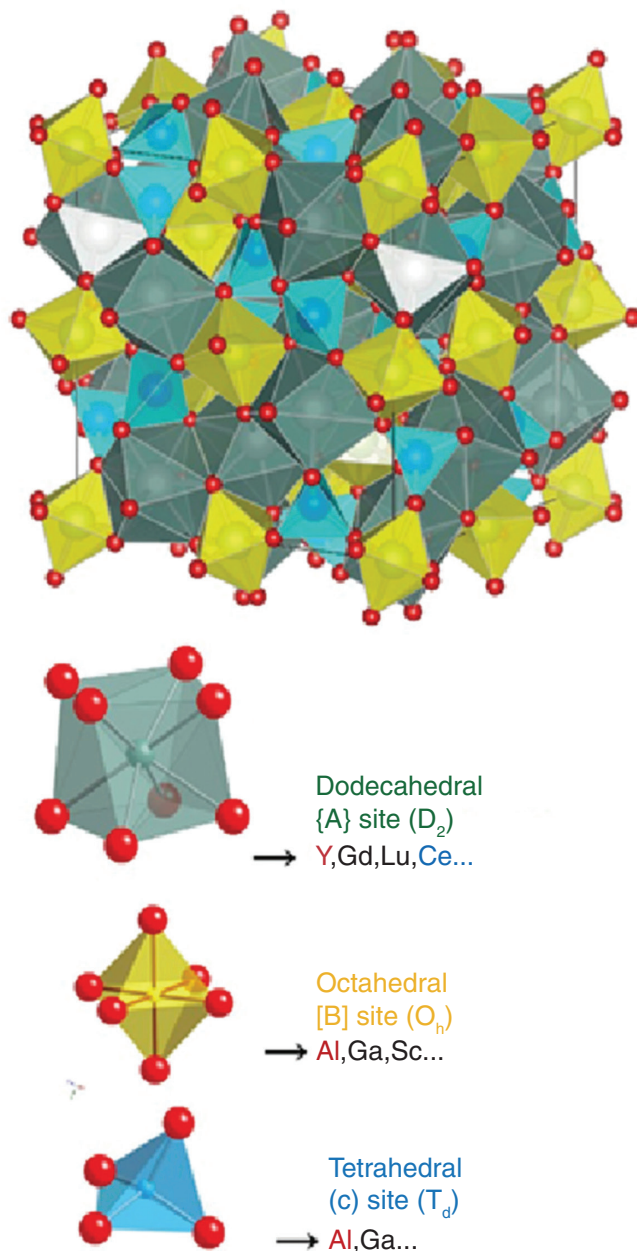


Fig. 8.6 Crystal structure and cation sites of garnet. Reproduced from (Ueda, 2015, b) with permission from the Journal of the Ceramic Society of Japan

On the basis of the strategy as shown in Section 4, we first optimized the energy gap between 5d and the CB. From the excitation wavelength and temperature dependence of photoconductivity measurements, we reported the relative energy location in the $Y_3Al_{5-x}Ga_xO_{12}:Ce^{3+}$ garnet phosphor, as shown in Fig. 8.7. With increasing Ga content, the energy of the $5d_1$ excitation level increases and the CB energy decreases. Thus, $Y_3Al_2Ga_3O_{12}:Ce^{3+}$ shows efficient electron transfer to the CB by blue excitation because of the optimum energy gap between the 5d level and the CB. In addition, $Y_3Al_2Ga_3O_{12}:Ce^{3+}$ shows good $Ce^{3+}:5d_1-4f$ luminescence, while $Y_3Ga_5O_{12}:Ce^{3+}$ does not show luminescence because the lowest 5d level is located within the CB. Therefore, $Y_3Al_2Ga_3O_{12}:Ce^{3+}$ can be regarded as a suitable candidate for a blue-light chargeable persistent phosphor. $Y_3Al_2Ga_3O_{12}:Ce^{3+}$ can act as a persistent phosphor if it has appropriate traps.

In general, to trigger persistent luminescence and improve the luminescence performance, a co-dopant ion is introduced into the phosphor for the creation of electron traps. A lanthanide ion is a good co-dopant for persistent phosphors,

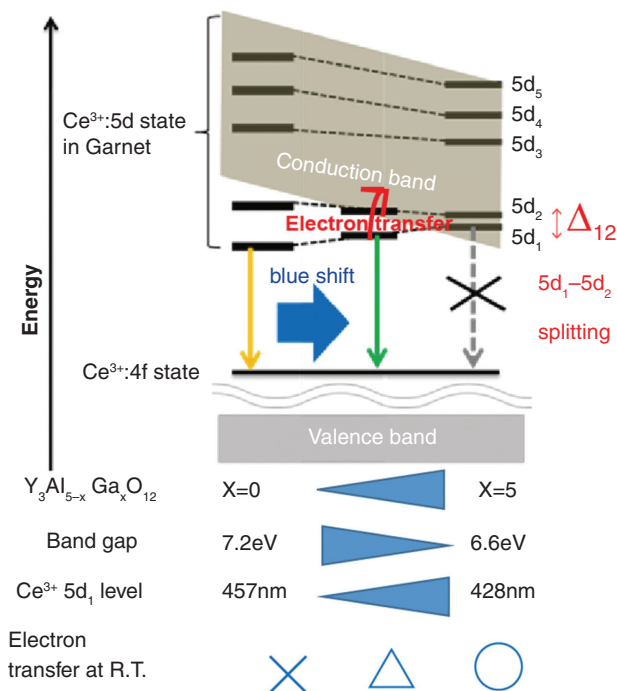


Fig. 8.7 Schematic energy diagram in $Y_3Al_xGa_{5-x}O_{12}:Ce^{3+}$. Reproduced from (Ueda, 2015, b) with permission from the Journal of the Ceramic Society of Japan

because some Ln^{3+} ions can capture an electron and then reduce to Ln^{2+} . For example, Dy^{2+} functions as an efficient electron-trapping center in $\text{SrAl}_2\text{O}_4:\text{Eu}^{2+}$ (Dorenbos, 2005; Dorenbos, 2013a; Dorenbos, 2013b). Vacuum referred binding energy (VRBE), introduced by Dorenbos, is a very useful parameter for discussing the electron trap depth (Dorenbos, 2005). Using the parameters in our study, a VRBE diagram of $\text{Y}_3\text{Al}_2\text{Ga}_3\text{O}_{12}$ was constructed, as shown in Fig. 8.8. When the VRBE of Ln^{2+} is located within the bandgap, Ln^{3+} can act as an electron trap. In $\text{Y}_3\text{Al}_2\text{Ga}_3\text{O}_{12}$, almost all the Ln^{2+} energy levels are located within the CB. There is a possibility that only Sm^{3+} , Eu^{2+} , Tm^{3+} , and Yb^{3+} can act as electron traps. In order to expand the options for co-dopants that can act as an electron trap, we focused on transition metals, which show multiple valence states. We found that Cr when used as a co-dopant significantly improves the persistent luminescence

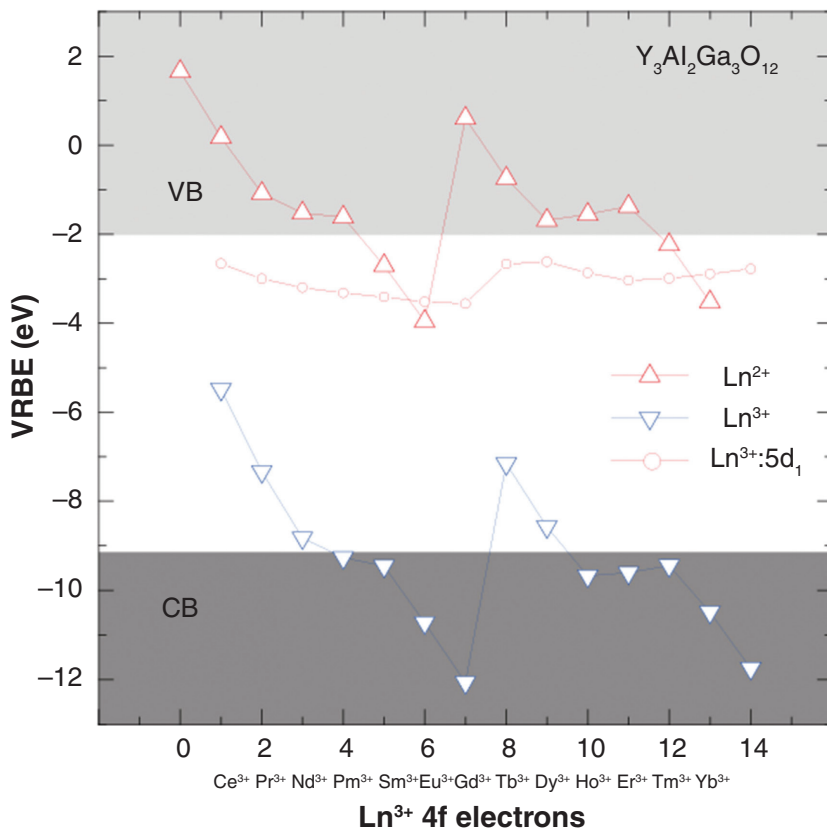


Fig. 8.8 VRBE diagram of $\text{Y}_3\text{Al}_2\text{Ga}_3\text{O}_{12}$. Reproduced from (Ueda, 2015, b) with permission from the Journal of the Ceramic Society of Japan

cence performance. The persistent luminance of $\text{Y}_3\text{Al}_2\text{Ga}_3\text{O}_{12}:\text{Ce}^{3+}\text{-Cr}^{3+}$ translucent ceramics observed 20 min after ceasing the 460 nm blue-light illumination is 208 mcd/m², which is much higher than that of the well-known $\text{SrAl}_2\text{O}_4:\text{Eu}^{2+}\text{-Dy}^{3+}$ compact powder, 96 mcd/m² (LumiNova GLL300FFS, Nemoto & Co., Ltd., Tokyo, Japan) (Ueda, 2014).

8.7 CB Engineering for Thermal Ionization and Trap Depth

We carried out extensive investigation on the charging and de-trapping properties of $\text{Y}_3\text{Al}_{5-x}\text{Ga}_x\text{O}_{12}:\text{Ce}^{3+}\text{-Cr}^{3+}$, for a wide range of Ga contents ($x = 0\text{--}5$) (Ueda, 2015). Fig. 8.9 shows the thermoluminescence excitation (TLE) or charging spectra recorded by monitoring the Ce^{3+} recombination luminescence in the $\text{Y}_3\text{Al}_{5-x}\text{Ga}_x\text{O}_{12}:\text{Ce-Cr}$ ($x = 0, 1, 2, 2.5, 3$) samples. In all the samples, TLE bands

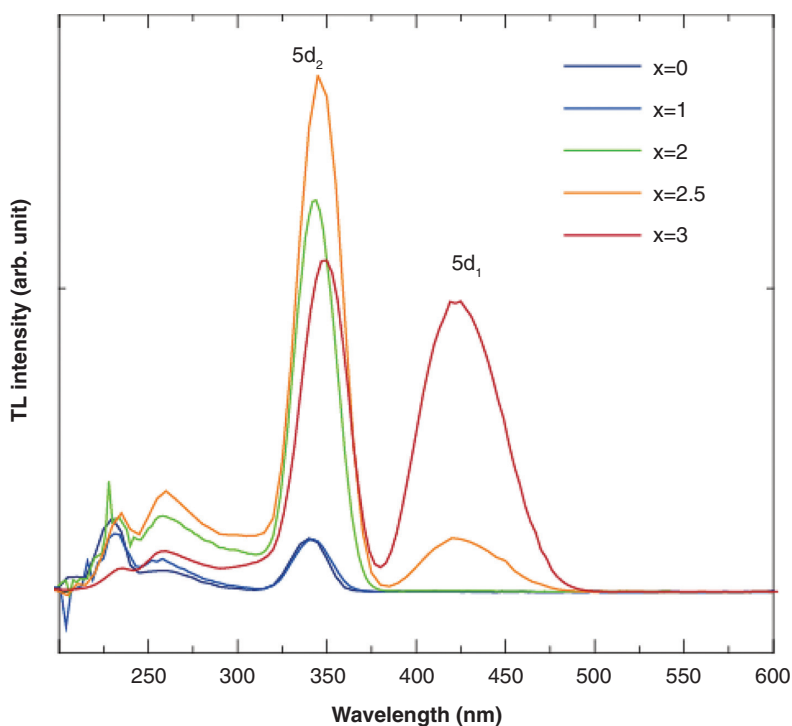


Fig. 8.9 Thermoluminescence excitation spectra of Ce-Cr-doped $\text{Y}_3\text{Al}_{5-x}\text{Ga}_x\text{O}_{12}$ samples (Ueda, 2015). Reproduced from (Ueda, 2015) with permission from the Royal Society of Chemistry

were observed at around 340, 270, and 230 nm. The band at 340 nm was attributed to the $4f-5d_2$ Ce^{3+} excitation. An intense TLE band attributed to the $4f-5d_1$ transition of Ce^{3+} appeared at around 420 nm, only in the $x = 2.5$ and 3 samples. These results show that samples with $x \geq 2.5$ can efficiently store electrons upon blue light illumination at room temperature. Thus, it is clear that the energy gap between the $5d_1$ level and the CB plays a critical role in effective blue light charging.

Normalized TL glow curves of the $Y_3Al_{5-x}Ga_xO_{12}:Ce-Cr$ samples after β -irradiation are shown in Fig. 8.10. The TL peak temperature can be controlled between 150 K and 400 K by varying the Ga concentration. The corresponding trap depths vary from 0.41 eV to 1.2 eV. From the VRBE diagram, it was found that with increasing Ga content, the absolute energy level of the trapped electron in Cr^{2+} remains almost the same, but the CB bottom energy decreases. Therefore,

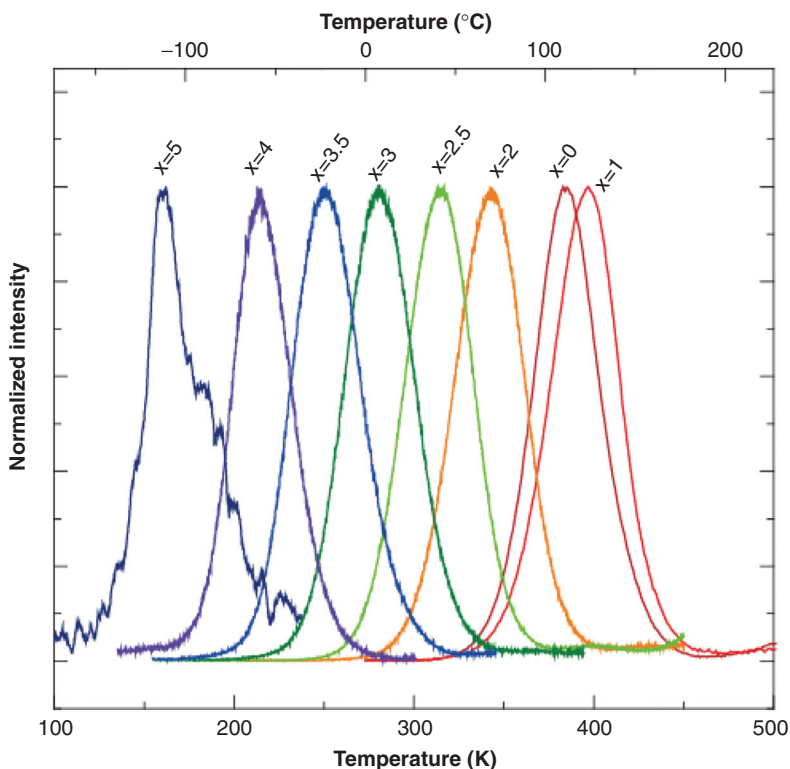


Fig. 8.10 Thermoluminescence glow curves at a heating rate of 10 K/min after β -irradiation of $Y_3Al_{5-x}Ga_xO_{12}:Ce-Cr$ samples with $x = 0, 1, 2, 2.5, 3, 3.5, 4,$ and 5 (Ueda, 2015). Reproduced from (Ueda, 2015) with permission from the Royal Society of Chemistry

de-trapping processes can be controlled by band gap engineering. Utilizing various trap depths, we realized not only persistent phosphors at room temperature, but also persistent phosphors that operate at low temperatures (-75°C for $x = 4$) and high temperatures (100°C for $x = 0$).

8.8 Color Tuning of Persistent Luminescence by Gd Substitution for Y

We have successfully developed new persistent ceramic phosphors, $\text{Y}_3\text{Al}_x\text{Ga}_{5-x}\text{O}_{12}$ (YAGG): $\text{Ce}^{3+}\text{-Cr}^{3+}$ ($x = 2.5, 3, 3.5$), with Ce^{3+} :*5d-4f* green luminescence ($\lambda_{\text{em}} = 505 \text{ nm}$) persisting for several hours after blue-light excitation,

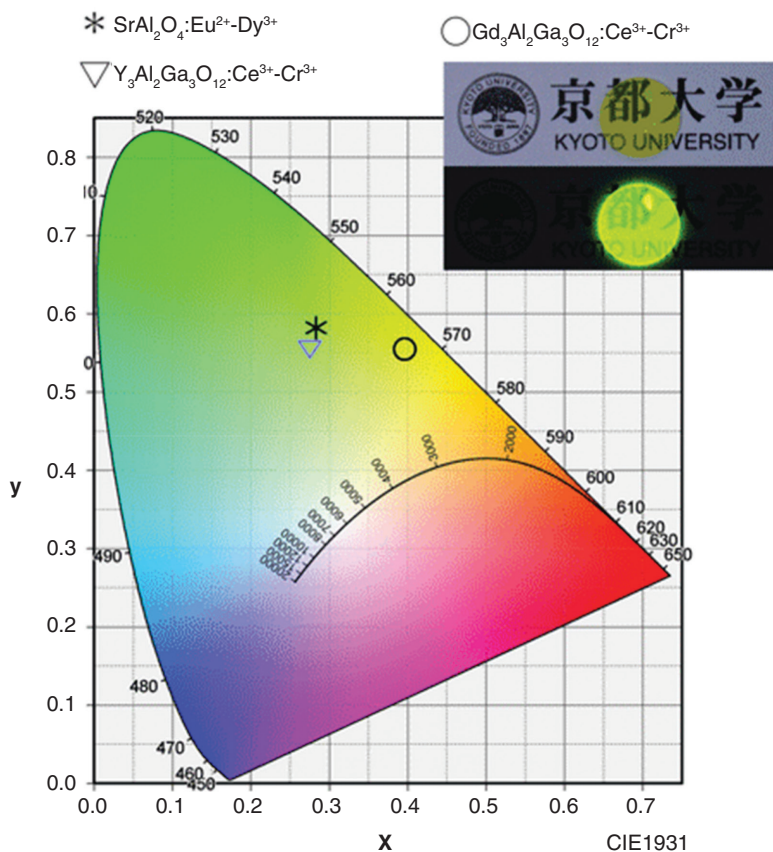


Fig. 8.11 Color chart for persistent luminescence of $\text{Gd}_3\text{Al}_2\text{Ga}_3\text{O}_{12}:\text{Ce}^{3+}\text{-Cr}^{3+}$, $\text{Y}_3\text{Al}_2\text{Ga}_3\text{O}_{12}:\text{Ce}^{3+}\text{-Cr}^{3+}$, and $\text{SrAl}_2\text{O}_4:\text{Eu}^{2+}\text{-Dy}^{3+}$ (Ueda, 2014, a). Reproduced from (Ueda, 2014, a) with permission from the Japan Society of Applied Physics

as shown in the previous section. However, the persistent luminescence color is almost the same as that of a well-known $\text{SrAl}_2\text{O}_4:\text{Eu}^{2+}\text{-Dy}^{3+}$ persistent phosphor. In order to realize longer persistent luminescence (yellow), a series of $\text{Gd}_3\text{Al}_{5-x}\text{Ga}_x\text{O}_{12}$ (GAGG) samples doped with Ce^{3+} and Cr^{3+} were selected. This is because, in garnet hosts such as $\text{Y}_3\text{Al}_{5-x}\text{Ga}_x\text{O}_{12}$, substitution of Y-sites by Gd ions leads to downshift of the $\text{Ce}^{3+}:5d_1$ level, and thus, redshift of the emission wavelength (Holloway, 1969; Tien, 1973; Blasse, 1967; Nishiura, 2011). Because the CB energy of GAGG referred to the vacuum level is almost the same as that of YAGG (Dorenbos, 2013), the Cr ions are expected to function as efficient electron traps in the GAGG host as well.

Fig. 8.11 shows the color chart for persistent luminescence of the $\text{Gd}_3\text{Al}_2\text{Ga}_3\text{O}_{12}:\text{Ce}^{3+}\text{-Cr}^{3+}$ transparent garnet ceramic phosphor. The persistent luminescence color of $\text{Gd}_3\text{Al}_2\text{Ga}_3\text{O}_{12}:\text{Ce}^{3+}\text{-Cr}^{3+}$ is more yellow than that of $\text{SrAl}_2\text{O}_4:\text{Eu}^{2+}\text{-Dy}^{3+}$ and $\text{Y}_3\text{Al}_2\text{Ga}_3\text{O}_{12}:\text{Ce}^{3+}\text{-Cr}^{3+}$ (Ueda, 2014, b). This is because the crystal field splitting strength increases upon substituting Y by Gd ions in $\text{Y}_3\text{Al}_2\text{Ga}_3\text{O}_{12}:\text{Ce}^{3+}\text{-Cr}^{3+}$. In addition, we successfully developed bluish green persistent luminescence in $\text{Lu}_3\text{Al}_2\text{Ga}_3\text{O}_{12}:\text{Ce}^{3+}\text{-Cr}^{3+}$ by controlling the crystal field splitting strength (Ueda, 2014, b).

8.9 Summary

We discussed the history of persistent phosphors in section 1, the basic information and development strategy for persistent phosphors in sections 2–4, and the properties of our developed persistent phosphors in sections 5–7. Till date, there have been no reports on the optimum energy location of the excited state of a luminescent center with respect to the CB for efficient charging of persistent phosphors at room temperature. In addition, there are only a few reports on the strategy used to control the electron transfer efficiency and the de-trapping temperature. We successfully developed a bright and long persistent phosphor by blue-light charging in $\text{Ln}_3\text{Al}_{5-x}\text{Ga}_x\text{O}_{12}:\text{Ce}^{3+}\text{-Cr}^{3+}$, based on the material design guide. The results of our study can serve as a guide for the development of persistent phosphors, although some trial and error would be involved. We are confident that our study would trigger the development of excellent persistent phosphors in the near future.

Acknowledgement

I would like to thank Professor Pieter Dorenbos, Delft University, Professor Andries Meijerink, Utrecht University, and Professor Setsuhisa Tanabe, Kyoto

University, for fruitful discussions on the research. This work was supported by Project of Strategic Young Researcher Overseas Visits Program for Accelerating Brain Circulation (International Network-hub for Future Earth: Research for Global Sustainability). I also wish to thank Professor Yoshizumi Kajii, Kyoto University, who was the Research Leader (B-3: Solar Light Storage Materials) in International Network-hub for Future Earth: Research for Global Sustainability.

References

- Aoki Y, Ishikawa M, Hirata Y, Sasai H, Oishi T, Takeuchi N, Takeuchi (1997) JP Patents 208948.
- Bettinelli M, Jungner H, Hölsä J (2012) *Eur J Mineral* 24: 885–890.
- Blasse G, Bril A (1967) *J Chem Phys* 47: 5139–5145.
- Bos AJJ, van Duijvenvoorde RM, van der Kolk E, Drozdowski W, Dorenbos P (2011) *J Lumin* 131: 1465–1471.
- Dorenbos P (2000a) *Phys Rev B* 62: 15640–15649.
- Dorenbos P (2000b) *Phys Rev B* 62: 15650–15659.
- Dorenbos P (2001) *Phys Rev B* 64: 125117.
- Dorenbos P (2002) *J Lumin* 99: 283–299.
- Dorenbos P (2005) *J Electrochem Soc* 152: 107–110.
- Dorenbos P (2013) *J Lumin* 134: 310–318.
- Dorenbos P (2013a) *Phys Rev B* 87: 035118.
- Dorenbos P (2013b) *J Lumin* 135: 93–104.
- Holloway JWW, Kestigian M (1969) *J Opt Soc Am* 59: 60–63.
- Jiang Z, Wang Y, Wang L (2010) *J Electrochem Soc* 157: J155–158.
- Korzhik MV, Trower WP (1995) *Appl Phys Lett* 66: 2327–2328.
- Lastusaari M, Laamanen T, Malkamäki M, Eskola KO, Kotlov Carlson AS, Welter E, Brito HF, Lin Y, Tang Z, Zhang Z (2001a) *Mater Lett* 51: 14–18.
- Lin Y, Tang Z, Zhang Z, Wang X, Zhang J (2001b) *J Mater Sci Lett* 2: 1505–1506.
- Lin Y, Tang Z, Zhang Z, Nan CW (2002) *Appl Phys Lett* 81: 996–998.
- Matsuzawa T, Aoki Y, Takeuchi N, Murayama Y (1996) *J Electrochem Soc* 143: 2670–2673.
- Murayama Y, *History of Persistent Phosphors in Japan* (日本夜光工業会, 2007).
- Murayama Y, Takeuchi N, Aoki Y, Matsuzawa T (1995) US Patents 5242006.

Nishiura S, Tanabe S, Fujioka K, Fujimoto Y (2011) IOP Conference Series: Materials Science and Engineering 18: 102005.

Setlur AA, Heward WJ, Gao Y, Srivastava AM, Chandran RG, Shankar MV (2006) Chem Mater 18: 3314–3322.

Shimizu T, Ueda J, Tanabe S (2012) Phys Stat Sol 9: 2296–2299.

Takasaki H, Tanabe S, Hanada T (1996) J Ceram Soc Jpn 104: 322–326.

Tien TY, Gibbons EF, DeLosh RG, Zacmanidis PJ, Smith DE, Stadler HL (1973) J Electrochem Soc 120: 278–281.

Ueda J, Aishima K, Nishiura S, Tanabe S (2011) Appl Phys Express 4: 042602.

Ueda J, Aishima K, Tanabe S (2013) Opt Mater 35: 1952–1957.

Ueda J, Dorenbos P, Bos AJJ, Kuroishi K, Tanabe S (2015) J Mater Chem 3: 5642–5651.

Ueda J, Kuroishi K, Tanabe S (2014a) Appl Phys Lett 104: 033519.

Ueda J, Kuroishi K, Tanabe S (2014b) Appl Phys Express 7: 062201.

Ueda J, Nakanishi T, Katayama Y, Tanabe S (2012) Phys Stat Sol 9: 2322–2325.

Wu JL, Gundiah G, Cheetham AK (2007) Chem Phys Lett 441: 250–254.

Yen WM, Shionoya S, Yamamoto H, *Phosphor handbook* (CRC Press/Taylor and Francis, 2007).

Zorenko Y, Voznyak T, Vistovsky V, Zorenko T, Nedilko S, Batentschuk M, Osvet A, Winnacker A, Zimmerer G, Kolobanov V, Spassky D (2007) Rad Meas 42: 648–651.